GEOPHYSICS, VOL. 55, NO. 9 (SEPTEMBER 1990); P. 1141–1147, 6 FIGS., 1 TABLE.

Transfer properties of the reduction of magnetic anomalies to the pole and to the equator

Károly I. Kis*

ABSTRACT

Reduction of magnetic anomalies to the magnetic pole and magnetic equator can be regarded as a linear transformation. The Hermitian transfer function characteristics of these transformations are discussed and improved using the Gaussian band–pass window. This procedure is of use in one– and two–dimensional cases. The application of the Gaussian band–pass window eliminates the finite discontinuity of the transfer function of reductions at zero frequency in all cases. The frequency band passed by the Gaussian window can be controlled by its parameters. Reduction to the equator can be used at low magnetic latitudes where reduction of two–dimensional anomalies to the pole has some instabilities caused by the infinite discontinuities of its transfer function. The windowed reductions are illustrated by their application to magnetic anomalies produced by two-dimensional and three-dimensional prisms.

INTRODUCTION

Reduction of magnetic anomalies to the pole is accepted as a standard procedure in the analyses of magnetic anomalies. It can be regarded as a linear transformation and has a Hermitian transfer function.

The procedure was initiated by Baranov (1957) and expanded by Baranov and Naudy (1964). The transformation has been discussed widely for both profile and gridded data. Bott et al. (1966) discussed Baranov's method based on Poisson's theorem. Shuey (1972) applied the Hilbert transformation for reduction of anomalies along the profiles. Blakely and Cox (1972a and 1972b) used the reduction for the identification of short polarity events in marine magnetic profiles. LeMouël et al. (1974) suggested a method for determination of coefficients for reducing of aeromagnetic profiles to the pole. Agocs (1986) used LeMouël's method for reduction of magnetic anomalies along profiles. Kanasewich and Agarwal (1970) suggested using the fast Fourier transform algorithm to make the method of Bhattacharyya (1965) more efficient. Syberg (1972) and Gunn (1975) presented the complex transfer function of reduction to the pole, while Silva (1986) formulated the reduction as a general linear inverse problem.

Some of the above mentioned papers pointed out that reduction to the pole has instabilities when applied to low–latitude magnetic anomalies. The procedure suggested by Baranov has a limit of $I > 30$ degrees and the version developed by Baranov and Naudy has a limit of its application to the anomalies $I > 16.5$ degrees. Silva stated that there is no practical use for reduction to the pole at latitudes less than 15 degrees.

TRANSFER PROPERTIES OF REDUCTION TO THE POLE IN THE CASE OF ANOMALIES ALONG A PROFILE

The complex transfer function of reduction to the magnetic pole can be expressed in the form

$$S_{T1}(f) = \frac{1}{Nn - Kk + j\,\mathrm{sgn}\,(f)(Nk + Kn)} \tag{1}$$

given by Blakely and Cox (1972a), and Shuey (1972); assuming a uniform direction of the source magnetization. In equation (1), f is the spatial frequency, sgn (f) is the sign of f, j is the imaginary unit; K, N, k, and n are the direction cosines of the magnetization and of the Earth's magnetic field respectively. The direction cosines can be expressed by the inclination α and declination β of the magnetization, and by the inclination I and declination D of the Earth's magnetic field:

$$K = \cos\alpha\cos(A - \beta), \qquad N = \sin\alpha,$$
$$k = \cos I\cos(A - D), \qquad n = \sin I, \tag{2}$$

where A is the azimuth of the profile measured clockwise from geographic north. The transfer function $S_{T1}(f)$ is not defined where its denominator is zero depending on the

Manuscript received by the Editor September 23, 1988; revised manuscript received February 20, 1990.
*Geophysics Department, Loránd Eötvös University, 1083 Budapest, Kun Béla tér 2, Hungary.

direction cosines; i.e., $Nn = Kk$ and $Nk = -Kn$, respectively. The transfer function $S_{T1}(f)$ is Hermitian. It has an even real part:

$$\mathrm{Re}\,\{S_{T1}(f)\} = \frac{Nn - Kk}{(Nn - Kk)^2 + (Nk + Kn)^2}, \tag{3}$$

and an odd imaginary part:

$$\mathrm{Im}\,\{S_{T1}(f)\} = \frac{-\mathrm{sgn}\,(f)(Nk + Kn)}{(Nn - Kk)^2 + (Nk + Kn)^2}. \tag{4}$$

The imaginary part of the transfer function has a discontinuity at $f = 0$. Its lower and upper limits are

$$\lim \mathrm{Im}\,\{S_{T1}(f)\} = \begin{cases} \dfrac{Nk + Kn}{(Nn - Kk)^2 + (Nk - Kn)^2} & \text{if } f \to -0, \\[2ex] \dfrac{-Nk - Kn}{(Nn - Kk)^2 + (Nk - Kn)^2} & \text{if } f \to +0. \end{cases} \tag{5}$$

The transfer properties of reduction in some special cases are as follows. If the magnetization and inclination of the Earth's magnetic field are vertical, $I = \alpha = \pm 90$ degrees (at the geomagnetic poles), the real part is unity, the imaginary part is zero, and the phase density spectrum also is zero. In this case, the reduction amounts to an identical transformation. If the magnetization and the Earth's magnetic field are horizontal, $I = \alpha = 0$ degrees (at the geomagnetic equator), the reduction depends on the angles $A - \beta$ and $A - D$. Where $A - \beta = i \times 90$ degrees or $A - D = i \times 90$ degrees ($i = \pm 1, \pm 3$), the transformation is not defined. Where $A - \beta = A - D = i \times 180$ degrees ($i = 0, \pm 1, \pm 2$), the real part is (-1), the imaginary part is 0 and the phase density spectrum also is zero.

In Figure 1 the real and imaginary parts of the reduction can be seen for the case of $I = \alpha = 60$ degrees, $D = \beta = 0$ degrees, and $A = 0$ degrees.

APPLICATION OF ONE-DIMENSIONAL FREQUENCY WINDOW

Reduction to the pole has the general properties of constant amplification of all frequencies, where the constant depends on the direction cosines and the finite discontinuity of the imaginary part at $f = 0$. Application of an appropriate frequency window can improve the transfer properties of the reduction. The frequency window should not modify the phase density spectrum, but it should decrease the constant amplification of the transfer function in the high frequency range and eliminate the finite discontinuity at $f = 0$.

The frequency window can be, among others, the Gaussian band-pass window proposed by Meskó (1984) which meets the requirements given above. The Gaussian window has the additional advantage that the product of signal-duration and frequency-bandwidth is minimum (Bracewell, 1965). The transfer function of the suggested band-pass window is as follows:

$$S_{BP}(f) = C\{\exp\,[-(36f/m_1)^2] - \exp\,\{[-(36f/m_2)^2]\}. \tag{6}$$

The normalization factor C is

$$C = \frac{1}{\exp\,[-(36f_{\max}/m_1)^2] - \exp\,[-(36f_{\max}/m_2)^2]}, \tag{7}$$

where

$$f_{\max} = \frac{m_1 m_2}{36}\left(\frac{2}{m_1^2 - m_2^2}\log\frac{m_1}{m_2}\right)^{1/2}. \tag{8}$$

The parameters m_1 and m_2 control the band passed by the Gaussian window and have the relation $m_1 > m_2$. If the lower and upper cutoff dimensionless frequencies f_L^c and f_U^c are defined as -3 dB amplification, then

$$f_L^c = 0.01635 m_1 \quad \text{and} \quad f_U^c = 0.01635 m_2. \tag{9}$$

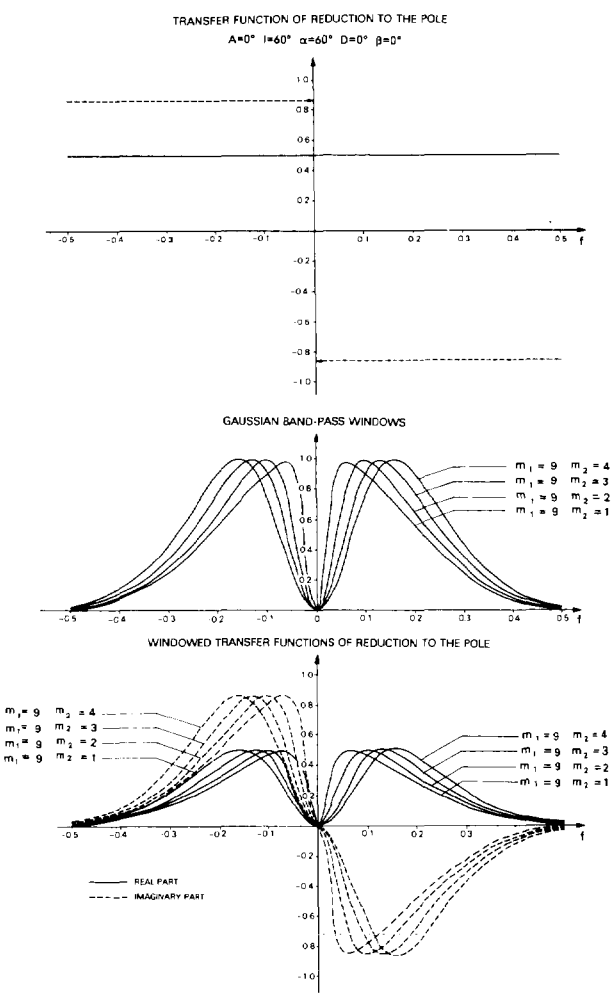

FIG. 1. Top: Real and imaginary parts of the 1-D transfer function of reduction to the magnetic pole for $I = \alpha = 60$ degrees, $D = \beta = 0$ degrees, $A = 0$ degrees. Middle: Transfer function of the 1-D Gaussian band-pass window controlled by the four different pairs of parameters $m_1 = 9$ and $m_2 = 1$, 2, 3, and 4. Bottom: Real and imaginary parts of the windowed transfer functions of reduction. The transfer functions are plotted versus the dimensionless spatial frequency f. Solid lines indicate the real parts and dashed lines indicate the imaginary parts.

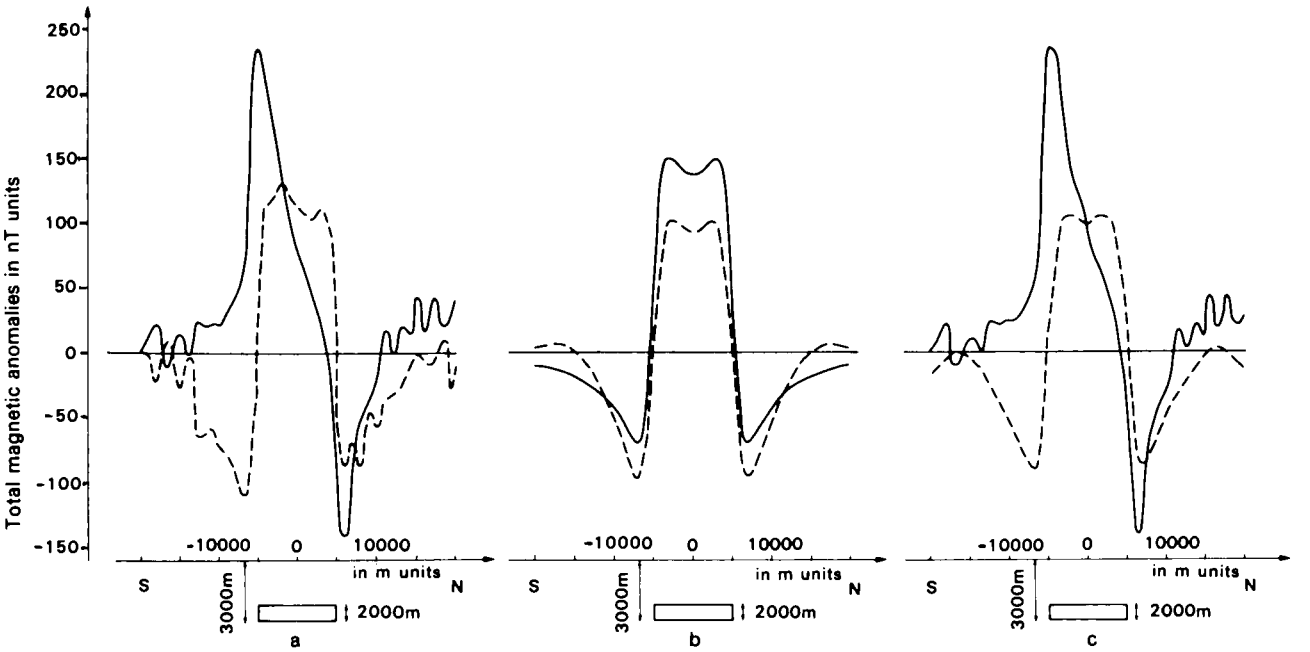

FIG. 2. Input and output of reduction to the pole: (a) Input consists of the anomaly produced by a 2-D prism, linear trend, and random numbers (solid line); anomaly reduced to the pole (dashed line); (b) Anomaly produced by a vertically magnetized prism (solid line) and its band–pass windowed anomaly (dashed line); (c) Input same as in (a) (solid line), result of reduction when the transfer function is band–pass windowed (dashed line).

The lower and upper cutoff spatial frequencies are given by

$$f_L^c/s \quad \text{and} \quad f_U^c/s, \tag{10}$$

where s is the sampling unit. Figure 1 shows four examples of Gaussian band–pass windows for four different pairs of parameters $m_1 = 9$ and $m_2 = 1, 2, 3$, and 4, respectively.

The transfer function of reduction is multiplied by the transfer function of the window

$$S_{T1}^{w}(f) = [\mathrm{Re}\,\{S_{T1}(f)\} + j\,\mathrm{Im}\,\{S_{T1}(f)\}]S_{BP}(f). \tag{11}$$

The application of the Gaussian band–pass window preserves the Hermitian property of the transfer function. Figure 1 also shows the real and imaginary parts of the transfer function of the reduction truncated by a band–pass window with the aforementioned pairs of parameters. With application of the band–pass window the anomalies reduced to the pole are band–pass filtered. The windowed transfer function is zero at $f = 0$, and hence windowing eliminates the direct component.

Figure 2 shows the results of model calculation along a north-south profile if the anomalies are produced by a two-dimensional (2-D) prismatic body whose magnetization is 1 A/m; the depths of the top and bottom of the 2-D prism are 1000 and 3000 m, respectively. The horizontal extent of the 2-D prism is 10 000 m; the magnetic directions are fixed by $I = \alpha = 60$ degrees and $D = \beta = 0$ degrees. Case (a) (Figure 2a) shows the anomaly that is produced by three effects: total anomaly of the 2-D prism, linear trend given by equation $T = 25 + 0.001x$, and random numbers between -20 and 20 nT with an average of 0. The result of reduction is influenced by the random noise and the linear trend. In this calculation the transfer function is given by the equation (1). The expected output shown in case (b) (Figure 2b) is not properly approximated. Case (b) illustrates the anomaly produced by the 2-D prism when $I = \alpha = 90$ degrees and its band–pass windowed anomaly controlled by the parameters $m_1 = 9$ and $m_2 = 1$. They are the expected outputs of reduction characterized by equations (1) and (11). Case (c) (Figure 2c) shows the model calculation when the input anomaly is the same as in case (a); the output of reduction

Table 1. Real part of $S_{T2}(\lambda)$ in the case of inclination $I = \alpha = 0$ degrees for declinations $D = 0$, 90, 180, and 270 degrees and $\beta = 0$, 90, 180, and 270 degrees.

	β			
D	0	90	180	270
0	$-\cos^{-2}\lambda$	$-\sin^{-1}\lambda\cos^{-1}\lambda$	$\cos^{-2}\lambda$	$\sin^{-1}\lambda\cos^{-1}\lambda$
90	$-\sin^{-1}\lambda\cos^{-1}\lambda$	$-\sin^{-2}\lambda$	$\sin^{-1}\lambda\cos^{-1}\lambda$	$\sin^{-2}\lambda$
180	$\cos^{-2}\lambda$	$\sin^{-1}\lambda\cos^{-1}\lambda$	$-\cos^{-2}\lambda$	$-\sin^{-1}\lambda\cos^{-1}\lambda$
270	$\sin^{-1}\lambda\cos^{-1}\lambda$	$\sin^{-2}\lambda$	$-\sin^{-1}\lambda\cos^{-1}\lambda$	$-\sin^{-2}\lambda$

corresponds to the band–pass windowed anomaly of the vertically magnetized 2-D prism.

TRANSFER PROPERTIES OF REDUCTION TO THE POLE FOR ANOMALIES MEASURED IN A GRID PATTERN

As in the previous case, assuming a uniform direction of source magnetization, the transfer function of reduction of total magnetic anomalies to the pole measured in a grid [in N–S and east-west (E-W) directions] follows:

$$S_{T2}(f_x, f_y) = \frac{f_x^2+f_y^2}{[N(f_x^2+f_y^2)^{1/2}+j(Lf_x+Mf_y)][n(f_x^2+f_y^2)^{1/2}+j(\ell f_x+mf_y)]} \tag{12}$$

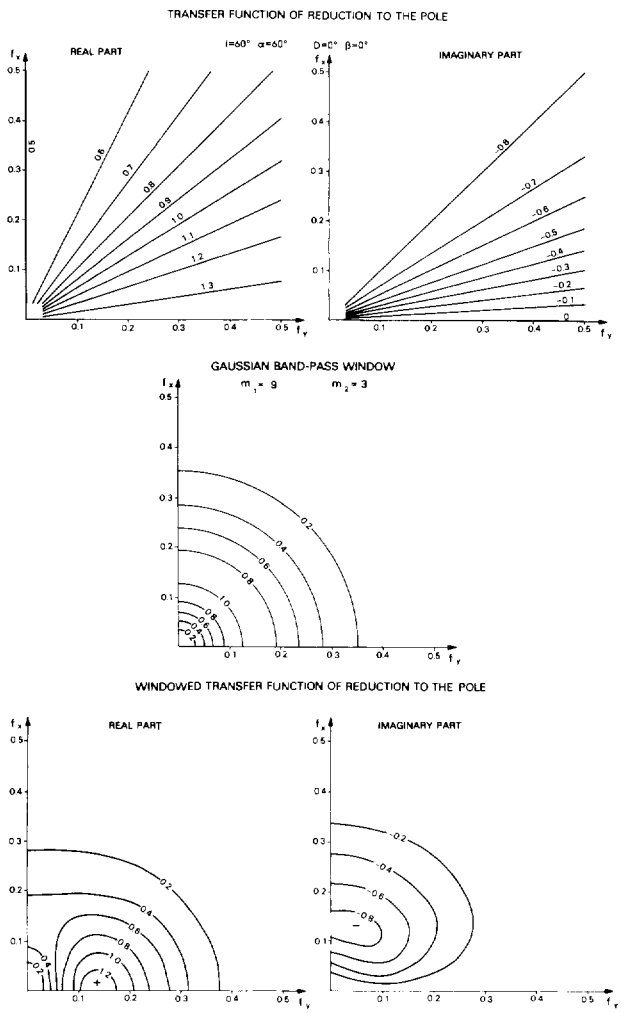

FIG. 3. Top: Real and imaginary parts of the 2-D transfer function of reduction to the magnetic pole for inclination $I = \alpha = 60$ degrees, and declination $D = \beta = 0$ degrees. Middle: Transfer function of the 2-D Gaussian band–pass window controlled by the pair of parameters $m_1 = 9$ and $m_2 = 3$. Bottom: Real and imaginary parts of the windowed transfer function of the reduction. The transfer functions are plotted versus the dimensionless spatial frequencies f_x and f_y.

[given by Gunn (1975)], where f_x and f_y are the spatial frequencies measured along the x–axis, which points to geographic north, and the y–axis, which points east. Direction cosines L, M, N and ℓ, m, n can be expressed by the inclination and declination of the magnetization and Earth's magnetic field, respectively

$$\begin{aligned} L &= \cos\alpha\cos\beta, & 1 &= \cos I\cos D,\\ M &= \cos\alpha\sin\beta, & m &= \cos I\sin D,\\ N &= \sin\alpha, & n &= \sin I. \end{aligned} \tag{13}$$

The transfer properties of the 2-D reduction can be given in polar coordinates if $f_x = f_r\cos\lambda$ and $f_y = f_r\sin\lambda$.

$$S_{T2}(\lambda) = \frac{1}{a_1\sin^2\lambda - a_2\sin\lambda\cos\lambda + a_3\cos^2\lambda + j(b_1\sin\lambda + b_2\cos\lambda)}, \tag{14}$$

where

$$\begin{aligned} a_1 &= Nn - Mm, & b_1 &= Mn + Nm,\\ a_2 &= M\ell + Lm, & b_2 &= Ln + N\ell,\\ a_3 &= Nn - L\ell. \end{aligned} \tag{15}$$

The transfer function $S_{T2}(\lambda)$ is independent of the radial distance since it varies only in the tangential direction. The real and imaginary parts of the transfer function are as follows:

$$\mathrm{Re}\{S_{T2}(\lambda)\} = \frac{a_1\sin^2\lambda - a_2\sin\lambda\cos\lambda + a_3\cos^2\lambda}{(a_1\sin^2\lambda - a_2\sin\lambda\cos\lambda + a_3\cos^2\lambda)^2 + (b_1\sin\lambda + b_2\cos\lambda)^2} \tag{16}$$

and

$$\mathrm{Im}\{S_{T2}(\lambda)\} = \frac{-b_1\sin\lambda - b_2\cos\lambda}{(a_1\sin^2\lambda - a_2\sin\lambda\cos\lambda + a_3\cos^2\lambda)^2 + (b_1\sin\lambda + b_2\cos\lambda)^2}. \tag{17}$$

The symmetry relations

$$\mathrm{Re}\{S_{T2}(\lambda + p\pi)\} = \mathrm{Re}\{S_{T2}(\lambda)\} \tag{18}$$

and

$$\mathrm{Im}\{S_{T2}(\lambda + p\pi)\} = (-1)^p\,\mathrm{Im}\{S_{T2}(\lambda)\} \tag{19}$$

demonstrate the Hermitian property of reduction to the pole where p is an integer number.

The transfer properties of reduction to the pole in some special cases are as follows. If the magnetization and the inclination of the Earth's magnetic field are vertical, i.e., $I = \alpha = \pm 90$ degrees (at the geomagnetic poles), the real part is unity and both the imaginary part and the phase density spectrum are zero. In this case the reduction is an identical

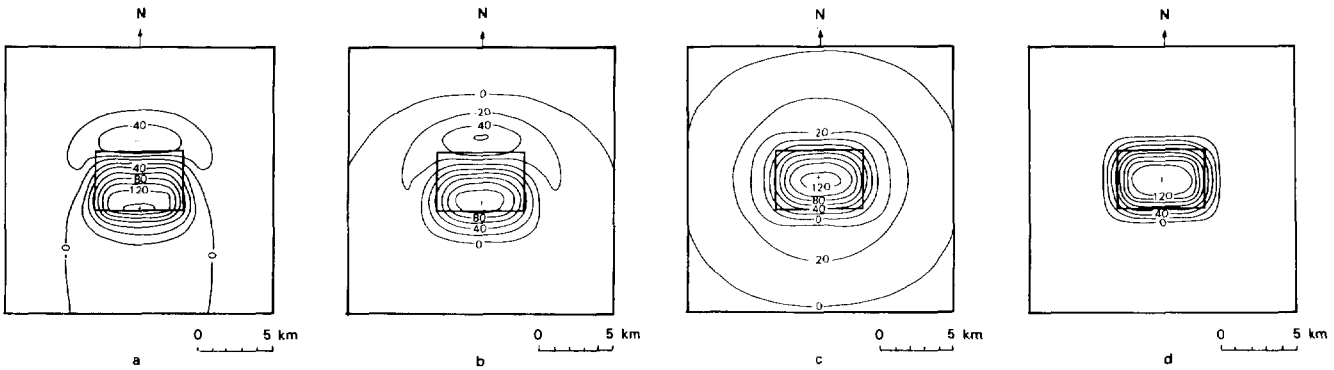

FIG. 4. Total magnetic anomalies produced by 3-D prism: (a) When $I = \alpha = 60$ degrees, $D = \beta = 0$ degrees; (b) Band–pass windowed anomalies of 3-D prism when $m_1 = 9$, $m_2 = 3$; (c) Band–pass windowed anomaly when $I = \alpha = 90$ degrees, $D = \beta = 0$ degrees as well as the output of the band–pass windowed reduction; (d) Anomaly when $I = \alpha = 90$ degrees, $D = \beta = 0$ degrees. Inner frame indicates the horizontal position of the 3-D prism. Contours are given in nT.

transformation. If the magnetization and the inclination of the Earth's magnetic field are horizontal, i.e., $I = \alpha = 0$ degrees (at the geomagnetic equator), the reduction depends on the angles D and β. Table 1 contains the real part of the transfer function in the case of $D = i \times 90$ degrees ($i = 0, 1, 2, 3$) and $\beta = j \times 90$ degrees ($j = 0, 1, 2, 3$). It can be seen that the limits of the transfer function become infinite along the f_x and/or f_y axes. This is the limit of the application of reduction to the pole in these cases. The imaginary part of the transfer function $S_{T2}(\lambda)$ is zero in this case. Except at the geomagnetic equator, the function $S_{T2}(\lambda)$ has different finite discontinuities at $f_x = f_y = 0$ depending on the direction of λ.

In Figure 3, the real and imaginary parts of the transfer function of the reduction to the pole can be seen for $I = \alpha = 60$ degrees and $D = \beta = 0$ degrees.

APPLICATION OF TWO–DIMENSIONAL FREQUENCY WINDOW

The elimination of finite discontinuities of the transfer function at the origin can be achieved by application of a proper frequency window. As in the previous case, a Gaussian band–pass window was applied. The 2-D Gaussian band–pass window corresponds to equations (6), (7), and (8) but, instead of f, the radial frequency f_r is used with

$$f_r = (f_x^2 + f_y^2)^{1/2}. \tag{20}$$

The parameters m_1 and m_2 control the band passed by the Gaussian window. The lower and upper cutoff frequencies can be expressed by equations (9) and (10). In Figure 3 the transfer function of the 2-D Gaussian band–pass window can be seen to be controlled by the pair of parameters $m_1 = 9$, $m_2 = 3$. The windowed transfer function of reduction is the following:

$$S_{T2}^{W}(f_x, f_y) = [\mathrm{Re}\,\{S_{T2}(f_x, f_y)\} + j\,\mathrm{Im}\,\{S_{T2}(f_x, f_y)\}]S_{BP}(f_r). \tag{21}$$

The real and imaginary parts of the windowed transfer function can be seen in Figure 3. The anomalies reduced to the pole are also band–pass windowed. The band–pass

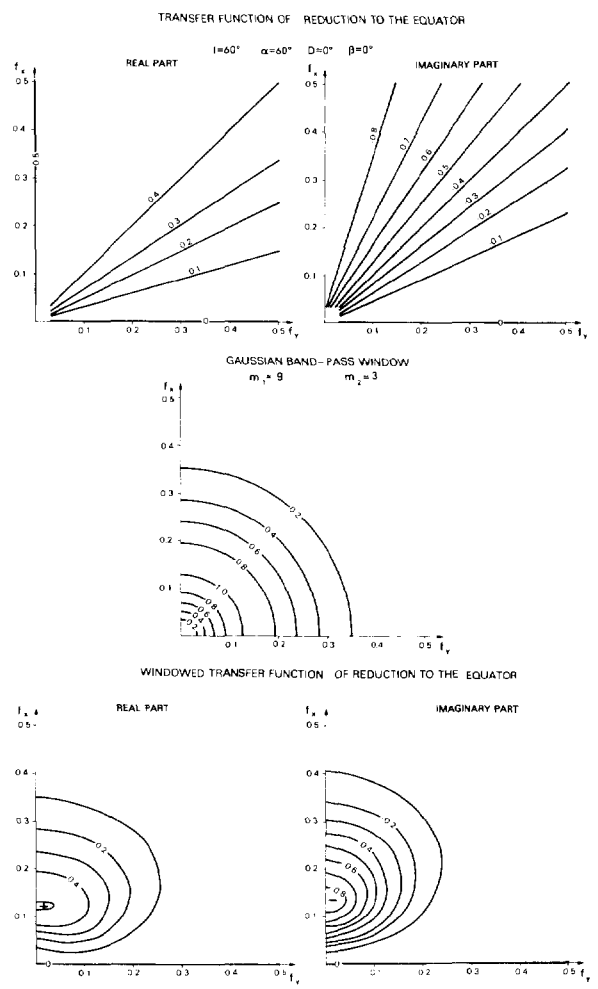

FIG. 5. Top: Real and imaginary parts of the 2-D transfer function of reduction to the magnetic equator for inclination $I = \alpha = 60$ degrees and declination $D = \beta = 0$ degrees. Middle: Transfer function of the 2-D Gaussian band–pass window controlled by the pair of parameters $m_1 = 9$ and $m_2 = 3$. Bottom: Real and imaginary parts of the windowed transfer function of reduction to the equator. The transfer functions are plotted versus the dimensionless spatial frequencies f_x and f_y.

window eliminates the finite discontinuity at $f_x = f_y = 0$ and, at the same time, decreases amplification in the higher frequency ranges. The windowing of the transfer function $S_{T2}(f_x, f_y)$ does not influence the phase density spectrum of the reduction. The band-pass windowed reduction to the pole is illustrated by model calculations shown in Figure 4; the anomaly produced by a 3-D vertical prism, where its magnetization is 1 A/m, the depth of the top and bottom are 1000 and 2000 m, and its horizontal extents are 4000 m (along the x-axis) and 6000 m (along the y-axis), respectively. The equations used are given by Whitehill (1973). Case (a) (Figure 4a) shows the total magnetic anomaly produced by the 3-D prism when $I = \alpha = 60$ degrees and $D = \beta = 0$ degrees. Case (b) (Figure 4b) presents its band-pass windowed anomaly controlled by the parameters $m_1 = 9$ and $m_2 = 3$. Case (c) (Figure 4c) depicts the band-pass windowed anomaly when $I = \alpha = 90$ degrees and $D = \beta = 0$ degrees, which would be the output of the band-pass windowed reduction to the pole. Case (d) (Figure 4d) illustrates the anomaly of the 3-D prism when $I = \alpha = 90$ degrees and $D = \beta = 0$ degrees.

The suggested windowed reduction to the pole was applied in the interpretation of field anomalies (Kis and Seiberl, 1989; Kis et al., 1989).

TRANSFER PROPERTIES OF REDUCTION TO THE EQUATOR FOR ANOMALIES MEASURED IN A GRID PATTERN

The transfer function of reduction to the equator can be derived as in the previous cases if the method suggested by Gunn (1975) is followed. Thus

$$S_{T3}(f_x, f_y) = \frac{\cos D \cos \beta f_x^2 + \sin (D + \beta) f_x f_y + \sin D \sin \beta f_y^2}{[N(f_x^2+f_y^2)^{1/2}+j(Lf_x+Mf_y)][n(f_x^2+f_y^2)^{1/2}+j(\ell f_x + mf_y)]} . \tag{22}$$

Reduction to the equator transforms the anomaly caused by any body with nonzero inclination into an anomaly that would be caused by the same body with zero inclination. The applied multiplier (-1) gives a maximum instead of a minimum above the sources.

The transfer properties can be investigated easily if the polar coordinates of the previous equations and constants are again initiated:

$$S_{T3}(\lambda) = S_{T2}(\lambda) [\sin D \sin \beta \sin^2 \lambda + \sin (D + \beta) \sin \lambda \cos \lambda + \cos D \cos \beta \cos^2 \lambda]. \tag{23}$$

The transfer function $S_{T3}(\lambda)$ breaks up into the real and imaginary parts

$$\mathrm{Re}\,\{S_{T3}(\lambda)\} = \mathrm{Re}\,\{S_{T2}(\lambda)\}[\sin D \sin \beta \sin^2 \lambda + \sin (D + \beta) \sin \lambda \cos \lambda + \cos D \cos \beta \cos^2 \lambda] \tag{24}$$

and

$$\mathrm{Im}\,\{S_{T3}(\lambda)\} = \mathrm{Im}\,\{S_{T2}(\lambda)\}[\sin D \sin \beta \sin^2 \lambda + \sin (D + \beta) \sin \lambda \cos \lambda + \cos D \cos \beta \cos^2 \lambda]. \tag{25}$$

It is evident from Equation (23) that the function $S_{T3}(\lambda)$ has only tangential dependence and is Hermitian.

The transfer properties of reduction to the equator in some special cases are as follows. If the magnetization and the Earth's magnetic field are horizontal, i.e., $I = \alpha = 0$ degrees (at the geomagnetic equator), the real part is -1, and the imaginary part is zero. The imaginary part has the point of removable discontinuities at $\lambda = \pi/2$ and $\lambda = 3\pi/2$. In this case, the transformation means a change of the sign of the anomaly; instead of a minimum, a maximum is obtained. If the magnetization and the Earth's magnetic field are vertical, i.e., $I = \alpha = \pm 90$ degrees (at the geomagnetic poles) the real parts depend on the angle λ. The real part varies between -1 and $+1$, and the imaginary part is zero.

Figure 5 shows the real and imaginary parts of the transfer

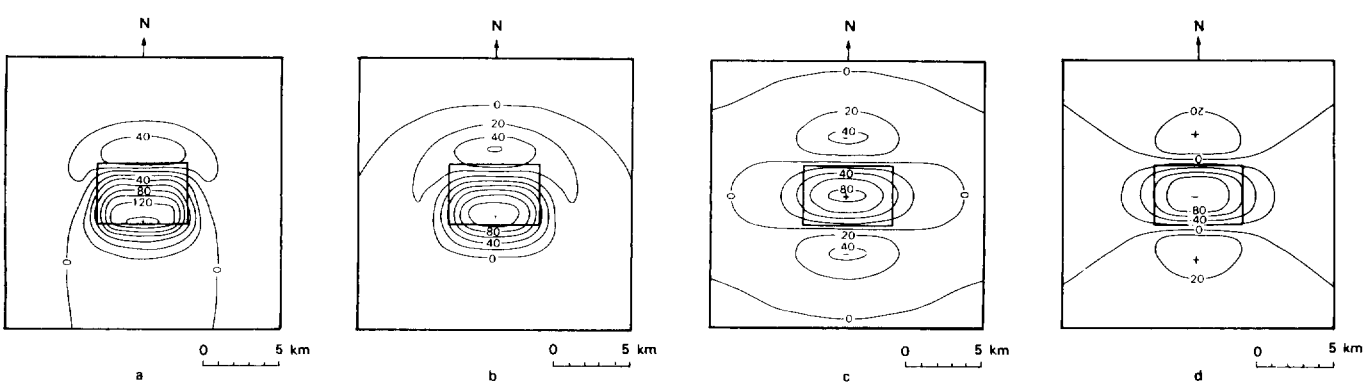

FIG. 6. Total magnetic anomalies produced by 3-D prism: (a) When $I = \alpha = 60$ degrees, $D = \beta = 0$ degrees; (b) Band-pass windowed anomalies when $m_1 = 9$, $m_2 = 3$; (c) Band-pass windowed reduction to the equator; (d) Anomaly when $I = \alpha = 0$ degrees and $D = \beta = 0$ degrees. Inner frame indicates the horizontal position of the 3-D prism. Contours are given in nT.

function $S_{T3}(\lambda)$ for the case $I = \alpha = 60$ degrees and $D = \beta = 0$ degrees.

As in the previous cases, application of the 2-D Gaussian band–pass window is also suggested. Figure 5 presents the transfer function of the Gaussian window ($m_1 = 9$ and $m_2 = 3$) and the band–pass windowed transfer function of reduction to the equator.

The band–pass windowed reduction to the equator is illustrated by model calculations shown in Figure 6. The model is the same as presented in Figure 4. Cases (a) and (b) show the same anomalies as in Figure 4. Case (c) is the band–pass windowed reduction to the equator, and case (d) illustrates the anomaly of the 3-D prism when $I = \alpha = 0$ degrees and $D = \beta = 0$ degrees.

ACKNOWLEDGMENT

The author wishes to thank Dr. W. B. Agocs for the encouragement and review of the manuscript.

REFERENCES

Agocs, W. B., 1986, Reduction to pole of magnetic profiles: Unpublished.

Baranov, V., 1957, A new method for interpretation of aeromagnetic maps: Pseudo–gravimetric anomalies: Geophysics, **22**, 359–383.

Baranov, V., and Naudy, H., 1964, Numerical calculation of the formula of reduction to the magnetic pole: Geophysics, **29**, 67–79.

Bhattacharyya, B. K., 1965, Two–dimensional harmonic analysis as a tool for magnetic interpretation: Geophysics, **30**, 829–857.

Blakely, R. J., and Cox, A., 1972a, Identification of short polarity events by transforming marine magnetic profiles to the pole: J. Geophys. Res., **77**, 4339–4349.

———, 1972b, Evidence for short geomagnetic polarity intervals in the early Cenozoic: J. Geophys. Res., **77**, 7065–7072.

Bott, M. H. P., Smith, R. A., and Stacey, R. A., 1966, Estimation of the direction of magnetization of a body causing a magnetic anomaly using a pseudo–gravity transformation: Geophysics, **31**, 803–811.

Bracewell, R., 1965, The Fourier transform and its application: McGraw–Hill.

Gunn, P. J., 1975, Linear transformations of gravity and magnetic fields: Geophys. Prosp., **23**, 300–312.

Kanasewich, E. R., and Agarwal, R. G., 1970, Analysis of combined gravity and magnetic fields in wavenumber domain: J. Geophys. Res., **75**, 5702–5712.

Kis, K., and Seiberl, W., 1989, The application of certain field transformation methods on the aeromagnetic data from the western part of the Viennese basin: Geophys. Trans., (in press).

Kis, K., Kloska, K., Kovács, F., and Tóth, S., 1989, Reduction to the magnetic pole of total field magnetic anomalies and determination of its parameters based on the Poisson's relation: Acta Geodaet., Geophys. et Montanist. Hung., **24**, 329–341.

LeMouël, J. L. Courtillot, V. E., and Gadeano, A., 1974, A simple formalism for the study of transformed aeromagnetic profiles and source location problems: J. Geophys. Res., **79**, 324–331.

Meskó, A., 1984, Digital filtering: Application in geophysical exploration for oil: Halsted Press.

Shuey, R. T., 1972, Application of Hilbert transforms to magnetic profiles: Geophysics, **37**, 1043–1045.

Silva, J. B. C., 1986, Reduction to the pole as an inverse problem and its application to low–latitude anomalies: Geophysics, **51**, 369–382.

Syberg, F. J. R., 1972, A Fourier method for the regional–residual problem of potential fields: Geophys. Prosp., **20**, 47–75.

Whitehill, D. E., 1973, Automated interpretation of magnetic anomalies using the vertical prism model: Geophysics, **38**, 1070–1087.